Merging of the islands of inversion at $N = 20$ and $N = 28$

E. Caurier,[1] F. Nowacki,[1] and A. Poves[2,3]
[1]*IPHC, IN2P3-CNRS and Université Louis Pasteur, F-67037 Strasbourg, France*
[2]*Departamento de Física Teórica and IFT-UAM/CSIC, Universidad Autónoma de Madrid, E-28049 Madrid, Spain*
[3]*Isolde (CERN) 1211 Genève 23, Switzerland*
(Received 1 April 2014; revised manuscript received 3 June 2014; published 10 July 2014)

The $N = 20$ and $N = 28$ "islands of inversion" are described by large scale shell model calculations with an extension of the interaction SDPF-U that makes it possible to mix configurations with different N$\hbar\omega$ or equivalently with different numbers of particles promoted from the sd shell to the pf shell. It allows to connect the classical sd-shell calculations below $N = 18$ with the sd (protons)-pf (neutrons) calculations beyond $N = 24$–26, for all the isotopes from oxygen to sulfur, using the same interaction. For some isotopes this range contains all the nuclei between the proton and the neutron drip lines and includes the $N = 20$ and $N = 28$ islands of inversion. We pay particular attention to the properties of the states at fixed N$\hbar\omega$ which turn out to be the real protagonists of the physics at $N = 20$. The existence of islands of inversion or deformation are explained as the result of the competition between the spherical mean field which favors the $0\hbar\omega$ configurations and the nuclear correlations which favor the deformed $N\hbar\omega$ configurations. The magnesium chain is exceptional because in it the $N = 20$ and $N = 28$ islands of inversion merge, enclosing all the isotopes between $N = 19$ and $N = 30$. Indeed, this would be also the case for the neon and sodium chains if their drip lines would reach $N = 28$.

DOI: 10.1103/PhysRevC.90.014302 PACS number(s): 21.60.Cs, 23.40.−s, 27.40.+z

I. INTRODUCTION

At the neutron rich edge, the structure of the spherical mean field may be at variance with the usual one at the stability line. The reason is that, at the stability line, the $T = 0$ channel of the nucleon-nucleon interaction has a stronger weight relative to the $T = 1$ channel than it has when the neutron excess is very large. If the spherical mean field gaps get reduced, open shell configurations, usually two neutron excitations across the neutron closure, take advantage of the availability of open shell protons to build highly correlated states that can be more bound than the closed shell configuration. Then the shell closure is said to have vanished. Although it has long been known that the ground state parity of ^{11}Be was at odds with the naive shell model picture [1], this fact was overlooked until much later, in connection with the discovery of halo nuclei with $N = 8$. Studies of charge radii, atomic masses, and nuclear spectra in the Mg and Na isotopic chains did show that a region of deformation exists around $N = 20$ below ^{34}Si. Key experimental references are gathered in Refs. [2–5]. Since then, a lot a experimental and theoretical work has ensued. Early mean field calculations suggested that deformation was responsible for the excess of binding of ^{31}Na [6], but at this stage to get a deformed minimum required the inclusion of *ad hoc* rotational corrections. In the framework of the shell model, the deformation in the region was soon associated with the dominance of two-particle–two-hole (2p-2h) excitations across the $N = 20$ shell gap between the normally occupied neutron $d_{3/2}$ orbit and the valence $f_{7/2}$ and $p_{3/2}$ orbits [7]. These configurations were dubbed intruders since they do not obey the normal filling of the standard spherical mean field. More recent shell model works include the Monte Carlo Shell Model (MCSM) calculations of the Tokyo group [8] and other large scale calculations in the sd-pf valence space [9]. Beyond mean field calculations have also been used in the description of the region with diverse degrees of success [10].

The interaction SDPF-U [11] that we proposed some time ago was aimed to describe the very neutron rich nuclei around $N = 28$ in a $0\hbar\omega$ space, with valence protons in the sd shell and valence neutrons in the pf shell. Therefore, it is applicable only to nuclei with $8 \leqslant Z \leqslant 20$ and $20 \leqslant N \leqslant 40$ and does not describe intruder states. The main asset of SDPF-U was the description of the vanishing of the $N = 28$ shell closure below ^{48}Ca, most notably in ^{42}Si [12] (a result which is now fully verified [13], but which produced initially some heated debates [14]). ^{42}Si was predicted to be oblate deformed and ^{40}Mg prolate deformed, exhibiting perhaps a neutron halo. Since its publication, it has been frequently used and shown to give an excellent description of this region of very neutron rich nuclei [15]. Very recently, these calculations were repeated in the same valence space with a somewhat different effective interaction, getting (as could be expected) very similar results [16]. As the sd part of SDPF-U is just the USD interaction [17] and its pf part a minor variant of KB3 previous to KB3G, it is appealing to complete SDPF-U with the sd-pf off-diagonal matrix elements and to retune the sd-pf cross shell monopoles in such a way that the SDPF-U results at $0\hbar\omega$ are mostly preserved and the sd-pf gaps are in accord with the experiment. This process results in the SDPF-U-MIX interaction. More details are given in the Appendix. The calculations are carried out using the codes ANTOINE and NATHAN [18] and reach basis dimensions of $O(10^{10})$. In a (very) loose sense one can pretend that this interaction covers the sector of the Segré chart $8 \leqslant Z, N \leqslant 40$. In this article we concentrate on the physics of the $N = 20$ "island of inversion" and its merging in some cases with the neighboring $N = 28$ one.

II. THE PHYSICS AT FIXED N$\hbar\omega$

What is the driving force behind the abrupt changes leading to the appearance of these islands of inversion? What makes

these intruder states special is that they need to be highly correlated in order to compensate for the energy loss associated to the breaking of the normal filling of the spherical mean field. Obviously, small gaps are easier to overcome; thus, a reduction of the neutron magic gaps at the very neutron rich edge is good news for the intruders. The mechanisms need not be the same in the different regions. For instance, in ^{11}Li the intruder is mostly pairing boosted while in ^{11}Be the quadrupole interaction is more important. In the other three neutron rich regions, $N = 20$, $N = 28$, and $N = 40$, the quadrupole interaction is the main player. Let us concentrate on the $N = 20$ case. Compared to the configurations with closed $N = 20$, the intruders (np-nh) have neutrons in open sd- and pf-shell orbits and in some cases protons in open sd-shell orbits. This favors the efficient buildup of correlations by the neutron-proton quadrupole interaction when the open orbits are the appropriate ones. And whose are these is dictated by the different variants of SU(3). For instance, when valence neutrons or protons occupy quasidegenerate orbits with $j_r - j_s = 2$ and $l_r - l_s = 2$ the coupling scheme is quasi-SU(3) [19], if they are in quasispin doublets the regime is that of pseudo-SU(3) [20]. In the limit of vanishing spin-orbit splitting, all the orbits in a harmonic oscillator shell form Elliott's SU(3) multiplet [21]. To get large coherence the neutrons and the protons must pertain to one or another of these coupling schemes. For example, in the case of the $N = 20$ intruders, the neutrons in the orbits $0f_{7/2}$ and $1p_{3/2}$, and the protons in $0d_{5/2}$ and $1s_{1/2}$, are in the quasi-SU(3) regime and the neutrons in $0d_{3/2}$ and $1s_{1/2}$ are in pseudo-SU(3).

Let us make these statement quantitative in a few selected cases. In this section all the calculations are performed at fixed $N\hbar\omega$. We only allow neutron jumps from the sd to the pf shell without any other truncation. We have verified that the effect of the proton excitations to the pf shell is negligible below $Z = 16$. We take care of the (small) center-of-mass contamination by adding to the effective interaction the center-of-mass Hamiltonian (with $\hbar\omega = A$). The expectation value of the center-of-mass Hamiltonian in the physical states is always below $0.001A$. The results for the low energy levels of ^{32}Mg are presented in Fig. 1. We can follow the evolution from the semimagic 0p-0h result, with a high excited 2^+ and a low

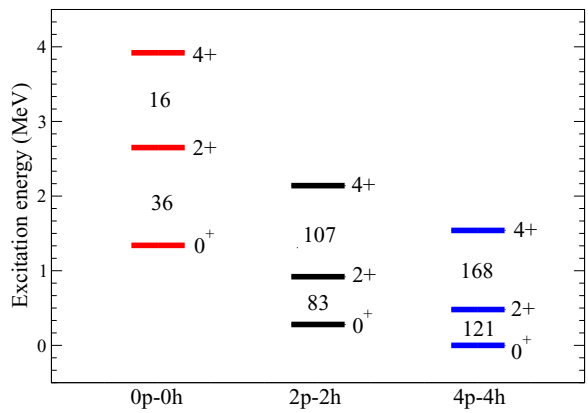

FIG. 1. (Color online) The low energy spectra and $B(E2)$'s (in e^2 fm^4) of the 0p-0h, 2p-2h, and 4p-4h configurations in ^{32}Mg.

$B(E2)$ to a rotational-like 2p-2h whose $B(E2)$ corresponds to $\beta = 0.4/0.5$ and finally to a perfect rigid rotor 4p-4h with $E(4^+)/E(2^+) = 3.2$ and a very large $B(E2)$ that corresponds to a superdeformed structure. Most important for our aims is that the gains in energy due to the correlations—defined as the difference between the energy which comes out of the diagonalization and the energy of the lowest 0^+ state of seniority zero in the corresponding space—are very different in the 0p-0h, 2p-2h, and 4p-4h spaces: 1.5, 12.5, and 21 MeV, respectively. These huge correlation energies may eventually overcome the spherical mean field gaps. In fact this is the case in ^{32}Mg. With SDPF-U-MIX the lowest 4p-4h 0^+ state is about 250 keV below the lowest 0^+ of the 2p-2h space and 1.2 MeV below the 0^+ of the 0p-0h configuration. This near degeneracy of the 2p-2h and 4p-4h bandheads is not a spurious manifestation of our spherical mean field not producing the right sd-pf gap; rather it is due to the fact that the energy gain per particle promoted to the pf shell is the same for both configurations. We want to stress again the fact that, in favorable circumstances like these, the gain in correlation energy of the intruders can beat the spherical mean field. In fact, in the laboratory frame, this is the microscopic mechanism responsible for the shape transitions from spherical to deformed nuclei [19]. The lowest negative parity state of 1p-1h nature is a 3^-, 4 MeV above the 2p-2h 0^+, and the lowest 3p-3h state is a 2^-, 2.5 MeV above the 2p-2h 0^+. Their respective energy gains are 5 and 16 MeV and the underlying structures correspond to the $K = 3^-$ and $K = 2^-$ bandheads as expected from the Nilsson diagrams for $\beta = 0.15$ and $\beta = 0.4$.

The 4p-4h state of ^{32}Mg has an academic interest in itself even if the states belonging to its rotational band do not manifest themselves openly in the low energy spectrum (as do their cousins in the superdeformed bands of ^{36}Ar and ^{40}Ca [22–24]) because of its strong mixing with the 0p-0h and 2p-2h spherical and deformed states. It may well happen that they could become yrast at some higher spin, but the threshold for neutron emission is not very high, and the experiments to find them are probably hopeless. In fact, one can understand semiquantitatively why this configuration can produce such superdeformed structure in the context of Elliott's SU(3) and its variants. Let us assume that the four pf-shell neutrons are in the quasi-SU(3) scheme and the four neutron holes in sd are in the pseudo-SU(3) scheme; in this case the neutrons contribute with $24b^2$ (times the effective charge) (where b is the harmonic oscillator length parameter) to the intrinsic quadrupole moment. If we go to the SU(3) limit in the pf-shell sector this number increases to $26b^2$. The value from the shell model calculation is $24.7b^2$. For the protons, the quasi-SU(3) limit gives $11b^2$ against $9.7b^2$ (times the effective charge) of the shell model calculation. With effective charges 0.46 and 1.31 for neutrons and protons, taken from the work of Dufour and Zuker [25], these values lead to $\beta = 0.6/0.7$ depending of the definition of β.

It follows from the above discussion that the configuration with four neutrons in the pf shell and two neutron holes in the sd shell maximizes the quadrupole moment and, *a fortiori*, the quadrupole correlation energy. Therefore, one should expect the 2p-2h configurations to be also dominant in ^{34}Mg. On the

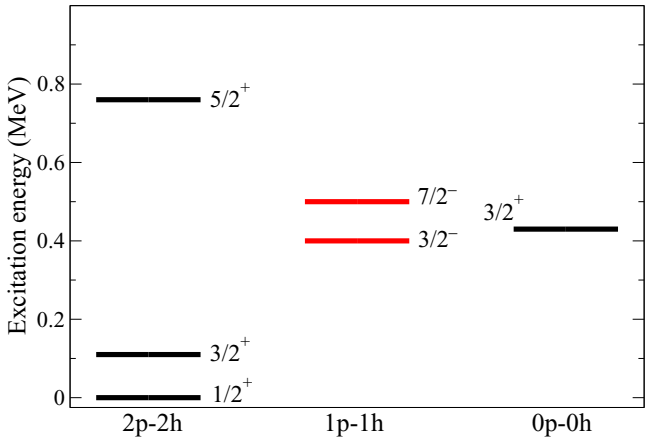

FIG. 2. (Color online) The low energy spectra of the 0p-0h, 1p-1h, and 2p-2h configurations in ^{31}Mg. Energies are relative to the 2p-2h $\frac{1}{2}^+$ state.

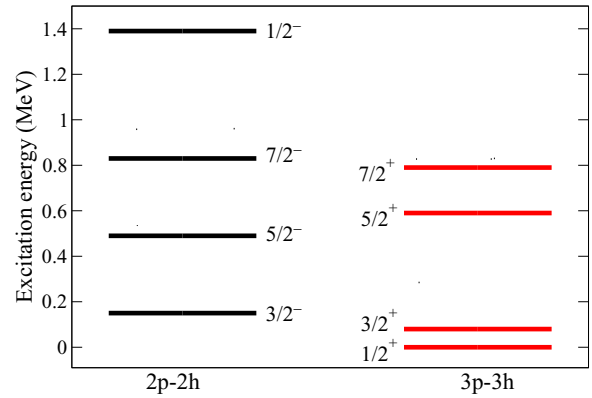

FIG. 3. (Color online) The low energy spectra of the 2p-2h and 3p-3h configurations in ^{33}Mg. Energies are relative to the 3p-3h $\frac{1}{2}^+$ state.

contrary, one expects the 0p-0h ones to begin taking over in ^{36}Mg. This would establish the limit of the $N = 20$ island of inversion. However, as we see in the next section, the very large depopulation of the $0f_{7/2}$ orbit in ^{36}Mg indicates that before leaving the $N = 20$ island of inversion we enter another, the $N = 28$ one, meaning that both islands are actually merged in a single one. These arguments apply as well to the 3p-3h excitations in the $N = 21$ isotopes, which we expect to be very low in energy.

In ^{31}Mg the configurations 0p-0h, 1p-1h, and 2p-2h are nearly degenerate. The lowest one is the 2p-2h configuration, which looks like a $K = \frac{1}{2}^+$ band, with an excited $\frac{3}{2}^+$ at $\sim$100 keV, in agreement with the experimental findings of Refs. [4]. The energy gain of the band is 14.5 MeV. The lowest 0p-0h state, a $\frac{3}{2}^+$, gains just 3.5 MeV and is 400 keV less bound than the 2p-2h $\frac{1}{2}^+$. The lowest 1p-1h negative parity state, a $\frac{3}{2}^-$, gains 8.5 MeV and is 400 keV above the 2p-2h $\frac{1}{2}^+$. These results are gathered in Fig. 2. The $E2$ and $M1$ transition probabilities of the 2p-2h band compare well with the recent experimental values from Ref. [26]:

$$B(M1)\left(\tfrac{5}{2}^+ \to \tfrac{3}{2}^+\right) = 0.1\text{–}0.5\mu_N^2 \ \left(\text{theor. } 0.35\mu_N^2\right),$$
$$B(M1)\left(\tfrac{3}{2}^+ \to \tfrac{1}{2}^+\right) = 0.019(4)\mu_N^2 \ \left(\text{theor. } 0.03\mu_N^2\right),$$
$$B(E2)\left(\tfrac{5}{2}^+ \to \tfrac{1}{2}^+\right) = 61(7)\ e^2\,\text{fm}^4 \ (\text{theor. } 84e^2\,\text{fm}^4).$$

The magnetic moment of the $\frac{1}{2}^+$ (using bare g factors) is $-0.85\mu_N$, very close to the experimental value $-0.88355(15)\mu_N$; thus, we can expect that its 2p-2h character is rather pure, the more so in view of the absence of nearby $\frac{1}{2}^+$ states to mix with. The intrinsic quadrupole moment of the ground state band is typical of this region, $Q_0 \approx 70\ e\ \text{fm}^2$.

In ^{33}Mg the lowest state at fixed configuration is the 3p-3h $\frac{1}{2}^+$, head of a $K = \frac{1}{2}^+$ band. At 150 keV appears the 2p-2h $\frac{3}{2}^-$, head of a $K = \frac{3}{2}^-$ band. The 0p-0h and 1p-1h states lie more than 1.5 MeV higher. These results are gathered in Fig. 3. Both structures are highly collective, with $B(E2)$'s in excess of 100 e^2 fm^4. In particular the $K = \frac{1}{2}^+$ 3p-3h band can be viewed as the addition of two neutrons to the ground state band of ^{31}Mg. It turns out that both bandheads, in spite of their different spin and parity, have negative magnetic moments ($-0.49\mu_N$ for the 2p-2h and -0.87 for the 3p-3h). Contrary to the assumption of Ref. [27], the magnetic moment of the $\frac{3}{2}^+$ 3p-3h state is positive ($+0.62\mu_N$). The results of the fully mixed calculation, which favor negative parity for the ground state, are discussed in Sec. VI.

Similar analysis can be carried out for all the remaining isotopes. We want to underline here two important points: (i) The configurations at fixed np-nh contain much of the relevant physics, and (ii) when configurations with different particle-hole structures, and hence with very different amounts of energy gains due to the correlations, compete, as is the case for the states of different parities in some $N = 19$ and $N = 21$ isotopes, the final balance between monopole energy losses and correlation gains is very delicate and the difficulty in accounting for experimental energy splittings between the positive and negative parity bands which may be smaller than 100 keV is extreme.

III. SPHERICAL MEAN FIELD VERSUS CORRELATION ENERGIES: THE MECHANISM OF CONFIGURATION INVERSION

As we have already anticipated, the islands of inversion occur when a group of adjacent nuclei have their ground states dominated by intruder configurations. We develop now the case of the $N = 20$ isotopes. We plotted in Fig. 4 the correlation energies of the lowest states of the 0p-0h and 2p-2h configurations. As the uncorrelated energy we take in each case the lowest diagonal energy (expectation value of the Hamiltonian) in a basis of states coupled to good J and with well defined generalized seniority. Because of this choice we incorporate in fact some diagonal pairing energy in our uncorrelated reference, but this is irrelevant for our purpose. As expected for semimagic nuclei, for the 0p-0h configurations, the correlation energies are small and roughly constant. On the contrary, for the 2p-2h intruders, they can be very large

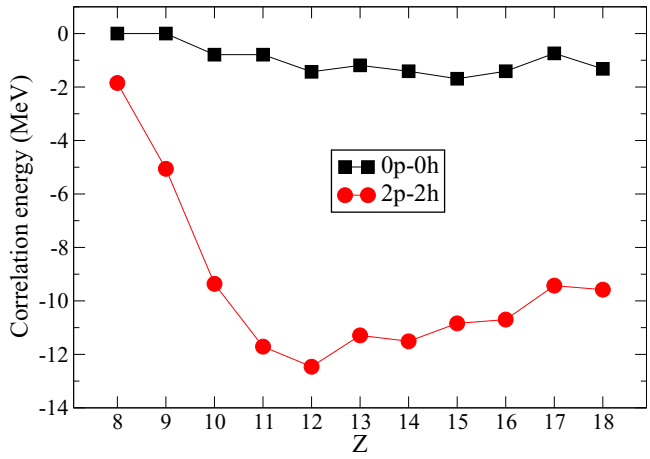

FIG. 4. (Color online) Correlation energies of the 0p-0h (squares) and 2p-2h (circles) configurations at $N = 20$.

and have a rapid variation with Z. The largest values occur at mid proton shell, when the quadrupole collectivity reaches its maximum.

In Fig. 5 we present the differences in energy between the lowest 0p-0h state with well defined J^π and the lowest 2p-2h state *without correlations*. It is seen that in all cases the normal filling gives the lowest energy, although between $Z = 8$ and $Z = 14$ there is an almost linear increase from 3 to 12 MeV, while from there on the curve is much flatter. This reflects the reduction of the sd-pf gap as we approach the neutron drip line. When we take fully into account the correlations the situation changes dramatically as reflected in the lower curve of the figure. The balance between the correlation gains and the monopole losses of energy defines the borders of the island of inversion at $N = 20$ in ^{29}F and ^{33}Al. Clearly, ^{30}Ne, ^{31}Na, and ^{32}Mg are bona fide members of the club. Equivalent graphs can be drawn for the other isotonic chains. Roughly speaking the

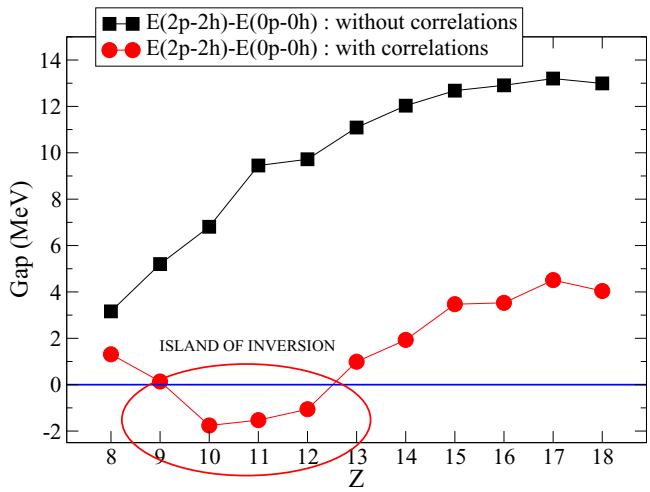

FIG. 5. (Color online) The gap between the 0p-0h and the 2p-2h configurations at $N = 20$, without correlations (squares) and including correlations (circles). Nuclei close to or below the zero line are candidates to belong to the island of inversion.

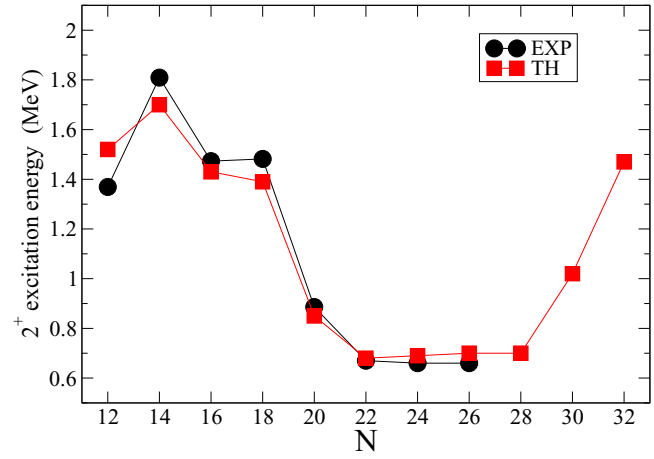

FIG. 6. (Color online) Excitation energies of the first 2^+ state in the magnesium isotopes. Results of the calculations with the SDPF-U-MIX interaction in the valence space of the sd shell for the protons and the sd-pf shells for the neutrons, compared with the available experimental data.

situation is very similar for the $N = 19$, $N = 21$, and $N = 22$ isotonic chains. It is probably not worthwhile to go much more beyond this qualitative definition of the somewhat fuzzy shores of the island of inversion around $N = 20$ because the predictions obtained in the analysis at fixed configuration may sometimes change when the full mixing is taken into account, the more so for the nuclei near to the borders. We are more precise in the section dealing with the full scale results of our calculations.

IV. FROM $N = Z$ TO $N = 32$ IN THE Mg, Ne, AND Si ISOTOPES

In Fig. 6 we compare the experimental 2^+ excitation energies of the even Mg isotopes, starting at $N = Z$, with the shell model calculations with the SDPF-U-MIX interaction. Up to $N = 16$ the results should not differ much from the ones produced by the USD interactions [17]. Beyond $N = 16$ the calculations include (if necessary for convergence) up to 6p-6h excitations from the sd shell to the full pf. The agreement is excellent and covers the span of isotopes from ^{24}Mg to the neutron drip line. Notice the disappearance of the semimagic closures at $N = 20$ and $N = 28$ and the presence of a large region of deformation which connects the two islands of inversion, previously thought to be split apart. The agreement is really superb. Beyond $N = 24$ the effect of the core excitations is perturbative and produces a small expansion of the spectra which improves slightly the agreement with the experimental data obtained in the $0\hbar\omega$ calculations. The merging of the $N = 20$ and $N = 28$ islands of inversion is evident.

In Fig. 7 we compare the $B(E2)$'s in the transition region with the experimental data including some unpublished results from RIKEN [28]. We use effective charges of 1.35 and 0.35 for protons and neutrons, respectively, which are fully compatible with a recent fit to the sd-shell nuclei with the interaction USD-A [29] and with the results obtained by

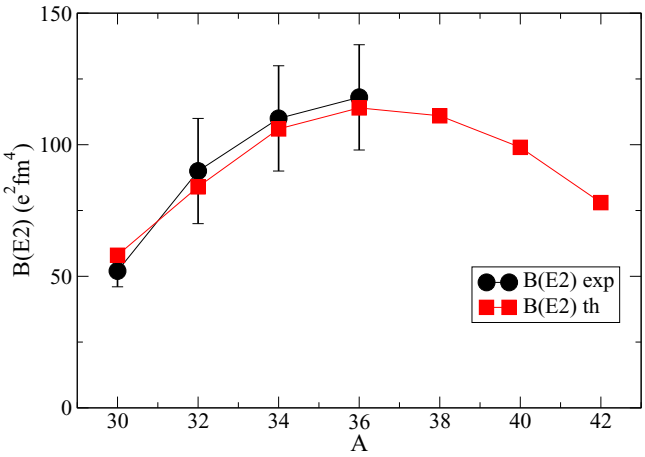

FIG. 7. (Color online) $B(E2)$'s of the magnesium isotopes compared to the experimental results.

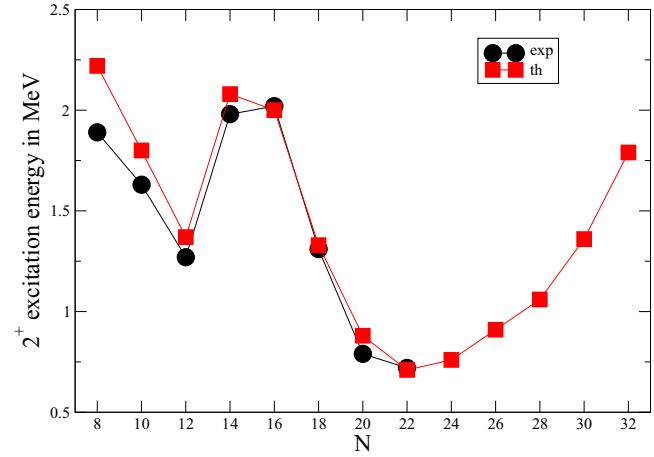

FIG. 9. (Color online) Excitation energies of the first 2^+ states in the neon isotopes (see caption of Fig. 6).

Dufour and Zuker in Ref. [25]. We take $\hbar\omega = 45A^{-1/3} - 25A^{-2/3}$. The agreement is very good as well.

In Fig. 8 we gathered the occupancies of the pf-shell orbits in the even-even magnesium isotopes. We aggregated the values of the f and p orbits for simplicity. The reference numbers for the total pf-shell occupancies are those labeled $0\hbar\omega$ in the figure. The pf shell has more than two neutrons in excess at $N = 20$ and $N = 22$. At $N = 24$ the excess is of about one neutron, and beyond that, the core excitations are much damped.

What is more interesting is that when the sd-shell core excitations become small, the occupancy of the p orbits (mainly $1p_{3/2}$) keeps increasing so that in $N = 26$ and $N = 28$ about two neutrons are in $1p_{3/2}$, whereas the expected occupancy if $N = 28$ were a strong closure would have been zero. In this sense we can speak of the merging of the islands of inversion at $N = 20$ and $N = 28$ in the magnesium isotopes. Notice also that a large occupancy of the p orbits favors the appearance of a neutron halo when the neutron separation energy becomes close to zero, as might be the case in ^{37,39}Mg and ^{40}Mg. Our occupancies for the pf-shell orbits in ^{32}Mg agree with the experimental results of Ref. [30].

The results for the neon isotopes (Fig. 9) are very similar to that for magnesium, although in this case the $N = 28$ isotope ^{38}Ne is most probably beyond the neutron drip line. The 2^+ excitation energy of ^{32}Ne is taken from Ref. [31]. In Fig. 10 we collected the occupancies of the f and p orbits in the isotopic chain as a function of the neutron numbers. The behavior is very similar to that in the magnesium chain, except that the p orbits are even more occupied. We have added the numbers for ^{31}Ne, because some recent experimental data [32] suggest that it could develop a neutron halo. Indeed, our results are consistent with this hypothesis because the $1p_{3/2}$ orbit has on average more than one neutron.

In Fig. 11 we show the results for the silicon isotopes (notice the very different energy scale). At variance with the magnesium case, we observe a majestic peak at $N = 20$, a

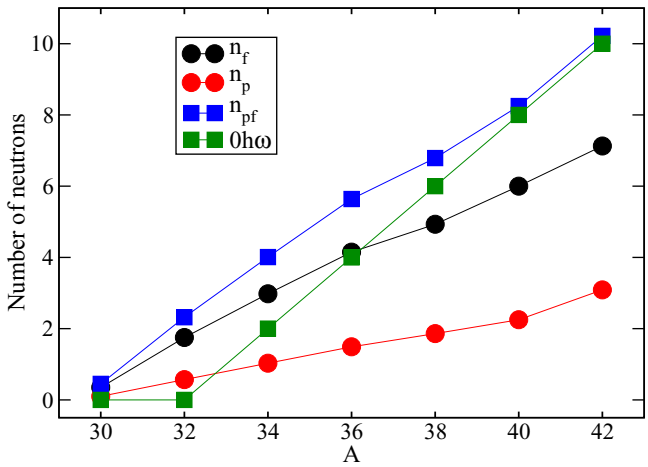

FIG. 8. (Color online) Occupation numbers of the pf-shell orbits in the magnesium isotopes; f orbits (black), p orbits (red), pf shell (blue), and normal filling (green).

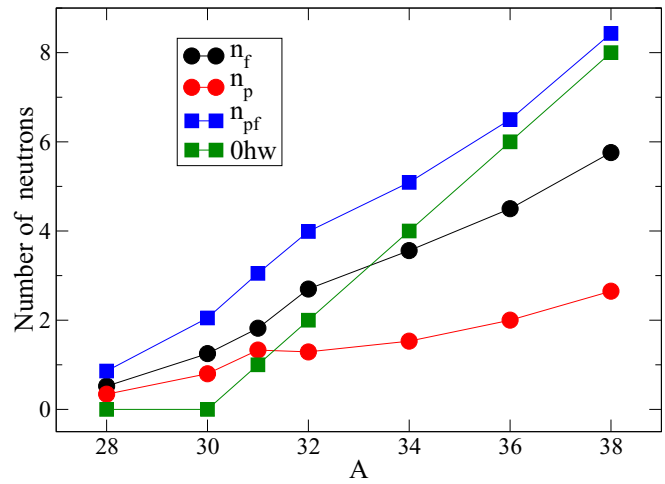

FIG. 10. (Color online) Occupation numbers of the pf-shell orbits in the neon isotopes: f orbits (black), p orbits (red), pf shell (blue), and normal filling (green).

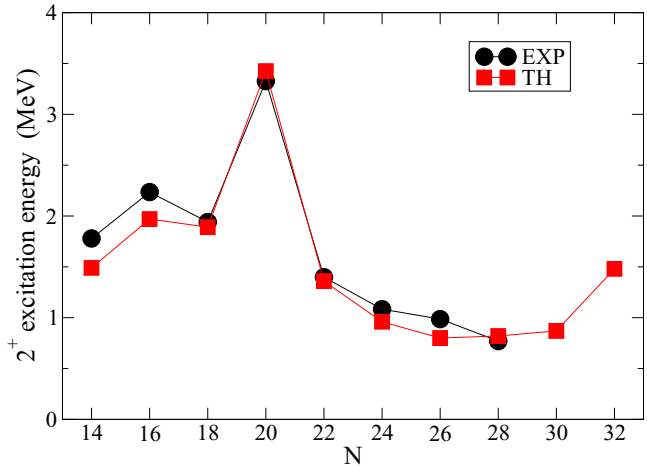

FIG. 11. (Color online) Excitation energies of the first 2^+ states in the silicon isotopes (see caption of Fig. 6).

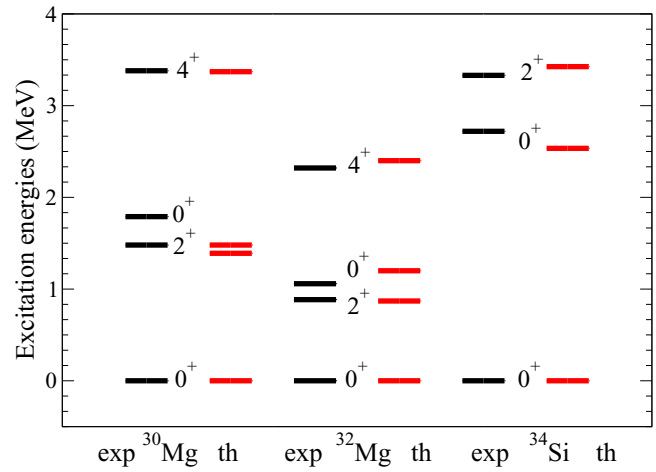

FIG. 12. (Color online) Comparison between experiment and theory for the most important low lying states in ^{30}Mg, ^{32}Mg, and ^{34}Si.

fingerprint of the double magic nature of ^{34}Si which we discuss in more detail later, and, as in the neon and magnesium cases, no trace of the $N = 28$ shell closure is seen, in agreement with the findings of recent experiments at GANIL [12] and RIKEN [13].

Some of these results were published in the proceedings of Ref. [33] but were mistakenly attributed to the SDPF-U-SI interaction; thus, we offer this erratum.

V. LANDING AT THE ISLAND OF INVERSION: ^{30}Mg $\rightarrow$ ^{32}Mg AND ^{34}Si $\rightarrow$ ^{32}Mg

There are two courses to land at the island of inversion by the ^{32}Mg shore: through the isotopic and the isotonic chains. Both are of paramount importance for the understanding of the rich variety of structural changes which take place in the region. Adding two neutrons to ^{30}Mg provokes the inversion of the normal and intruder configurations which are shifted by nearly 3 MeV in ^{32}Mg. In the isotonic course the transition is even more abrupt, as was recently shown in a GANIL experiment [34]: by removing two protons from ^{34}Si, the intruder (deformed) state is shifted down by about 4 MeV with respect to the spherical one to become the ground state of ^{32}Mg.

We compare the experimental data with the shell model results in Fig. 12. The calculations include configurations with up to six neutrons in the pf shell. ^{30}Mg and ^{34}Si have ground states which are dominantly (>80%) 0p-0h and first excited 0^+'s dominantly 2p-2h. They differ in the structure of the lowest 2^+ which is 0p-0h in ^{30}Mg and 2p-2h in ^{34}Si. More details on this last nucleus can be found in Ref. [34], where a close to final version of SDPF-U-MIX was utilized.

The structure of the 0^+ states in ^{32}Mg is extremely singular; the ground state has 9% 0p-0h, 54% 2p-2h, 35% 4p-4h, and 1% 6p-6h; thus, it is a mixture of deformed and superdeformed shapes. The excited 0^+ state has 33% 0p-0h, 12% 2p-2h, 54% 4p-4h, and 1% 6p-6h, a surprising hybrid of spherical and superdeformed shapes, whose direct mixing matrix element is strictly zero. One could fancy to name it the *shape entangled state*.

The 2^+ state has a structure similar to the ground state. As shown in Fig. 7 its $B(E2)$ agrees with the experimental result. In addition, the calculated spectroscopic quadrupole moments of the 2^+ and 4^+ states and the $B(E2)$'s in the yrast band are compatible with a single intrinsic state with $Q_0 \approx 65$ e fm^2. The MCSM calculations of Ref. [8], which only include the $0f_{7/2}$ and $1p_{3/2}$ orbits of the pf shell, give results similar to ours except for the excited 0^+ state, which is too high by almost 2 MeV. Similarly, in $^{34-40}$Mg the calculated $E2$ properties are compatible with $Q_0 \approx 70$ e fm^2, which is another fingerprint of the merging of the $N = 20$ and $N = 28$ islands of inversion or deformation.

Since the early β-decay experiments at Isolde [35] it is known that in ^{32}Mg there are many states, mostly of negative parity, above the 4^+ state. They have been explored more recently via the ^{32}Na β decay [27,36] or in (p,p') experiments [37]. Reference [27] presents also the MCSM predictions for the negative parity states fed in the β decay. The experimental level at 2.551 MeV is most probably the second 2^+ state. MCSM puts it at 3 MeV, whereas we get it at nearly the same energy as the 4^+ state. According to these references, the lowest experimental negative parity state would appear at 2.858 MeV. The calculated negative parity states are 1^- at 3.0 MeV, 2^- at 3.1 MeV, 3^- at 3.4 MeV, 4^- at 3.9 MeV, 0^- at 4.0 MeV, and 5^- at 4.2 MeV. They are mostly of 3p-3h nature. The lowest negative parity states in the MCSM description are of 3p-3h nature as well, and start at 3.8 MeV with four close packed states (2^-, 1^-, 2^-, 3^-) followed by a doublet (4^-, 5^-) at about 4.5 MeV.

VI. MISCELLANEOUS RESULTS

A. ^{31}Mg and ^{33}Mg

The $N = 19$ and $N = 21$ isotonic chains are very complex, because of the near degeneracy of configurations with different particle-hole structure, as discussed in Sec. II. In ^{31}Mg the

TABLE I. Excitation energies (in MeV) and magnetic moments (in μ_N) for the low lying states of ^{31}Mg and ^{33}Mg with (b)are and (e)ffective g factors.

	J^π	E (expt.)	E (theor.)	μ (theor.) (b)	μ (theor.) (e)
^{31}Mg	$\frac{1}{2}^+$	0.0	0.04	–0.93	–0.65
	$\frac{3}{2}^+$	0.05	0.04	+1.13	+0.81
	$\frac{3}{2}^-$	0.221	0.0	–1.24	–1.07
^{33}Mg	$\frac{3}{2}^-$	0.0	0.0	–0.54	–0.49
	$\frac{5}{2}^-$	0.484	0.33	–0.07	–0.09
	$\frac{1}{2}^+$		0.04	–0.93	–0.69
	$\frac{3}{2}^+$		0.12	+0.69	+0.44

situation is especially critical. We have not tried to fine-tune the interaction to improve our results which amount to having the $\frac{1}{2}^+$, $\frac{3}{2}^+$, and $\frac{3}{2}^-$ states degenerated (see Table I). The magnetic moment of the $\frac{1}{2}^+$ ground state was measured as $-0.88355(15)\mu_N$ [4]. Our predictions show a very strong dependence on the choice of the gyromagnetic factors and marginally agree with the experimental value.

In ^{33}Mg the fully mixed calculation produces a $\frac{3}{2}^-$ ground state with the $\frac{1}{2}^+$ state just 40 keV higher. The magnetic moment of the $\frac{3}{2}^-$, $-0.54\mu_N$ (b), $-0.49\mu_N$ (e), is short from the experimental value, $-0.7456(5)\mu_N$. If the $J = 3/2$ experimental assignment is firm, then positive parity is excluded by the sign of the magnetic moment. Notice, however, that our results locate the positive parity states almost degenerated with the ground state. The magnetic moment of the 4p-4h $\frac{3}{2}^-$ state is $-1.67\mu_N$ (bare) [$-1.36\mu_N$ (effective)]; therefore, a somewhat larger mixing of 4p-4h components than that given by our calculation may line up the theoretical value with the experimental one.

B. ^{31}Na and ^{33}Na

^{31}Na was for many years the protagonist of the $N = 20$ saga, even if only the properties of its ground state were known (spin parity, magnetic moment, isotope shift, binding energy). Although other nuclei have taken up the relay nowadays, it still deserves attention. We have gathered the available experimental information in Fig. 13. The newest data [38,39] consist of the excitation energies of two members of the $K = \frac{3}{2}^+$ ground state rotational band and the $B(E2)$ of the lowest in-band decay in ^{31}Na, and the excitation energies of two levels in ^{33}Na. Notice the very nice agreement of the calculation and the data which extends to the ground state magnetic moment [$2.298\mu_N$ (experiment) vs the calculated $2.26\mu_N$ (b) or $1.96\mu_N$ (e)]. As in the ^{32}Mg case the calculated $E2$ properties of ^{31}Na are compatible with an intrinsic state with $Q_0 \sim 65\ e$ fm^2. We have also plotted the results for ^{33}Na in which the behavior of the calculated excitation energies is closer to $J(J+1)$ than in the previous case, and $Q_0 \sim 72\ e$ fm^2. The comparison of the new data with the calculated values is quite good and supports strongly a $\frac{3}{2}^+$ ground state.

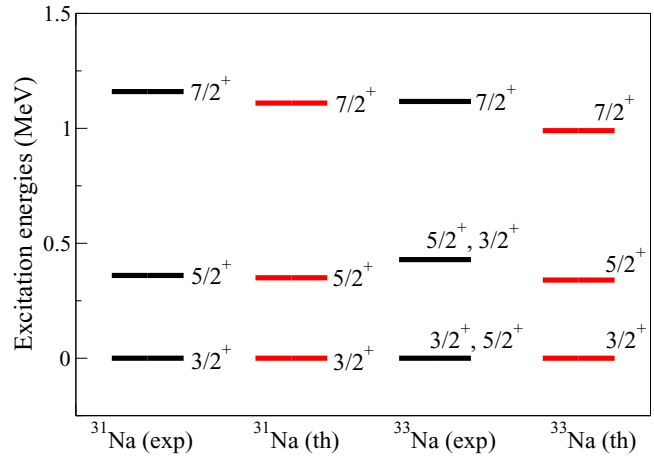

FIG. 13. (Color online) Comparison of the calculated spectra with the available experimental data in ^{31}Na and ^{33}Na.

C. ^{30}Ne, ^{31}Ne, and ^{32}Ne

To complete this spectroscopic tour, we visit the neon chain. Our results for ^{30}Ne, 2^+ at 0.79 MeV and 4^+ at 2.14 MeV, compare very well with the experimental values, 0.792 and 2.235 MeV, respectively. The $B(E2)$, $(2^+ \rightarrow 0^+)$ is predicted at 66 e^2 fm^4 compared with the measured value 90(54) e^2 fm^4. Again a single intrinsic state with $Q_0 \sim 60\ e$ fm^2 explains the calculated $E2$ properties. ^{32}Ne is more deformed: $Q_0 \sim 65\ e$ fm^2. The calculated 2^+ excitation energy, 0.67 MeV, fits well with the experimental value, 0.72 MeV. The 4^+ is predicted at 1.89 MeV. Finally, for ^{31}Ne the calculation produces a $\frac{3}{2}^-$ ground state which is mainly 2p-2h, and the first excited state at ~200 keV is a $\frac{3}{2}^+$ of 3p-3h character, belonging to the $K = \frac{1}{2}^+$ in parallel with what happens in its isotone ^{33}Mg. The intrinsic quadrupole moment of the $K = \frac{3}{2}^-$ band is $Q_0 \sim 60\ e$ fm^2, and, as we mentioned before, the occupation of the p orbits exceeds 1.2 neutrons.

D. ^{29}F and ^{31}F

Not very much is known experimentally about ^{29}F and ^{31}F. Our calculations produce a $\frac{5}{2}^+$ ground state in ^{29}F, which is 60% $0\hbar\omega$ with a first excited $\frac{1}{2}^+$ at 0.91 MeV, which is 80% intruder and the head of a $K = \frac{1}{2}^+$ band, as expected from quasi-SU(3) and Nilsson diagrams. This compares fairly well with a recent measure at RIKEN [40], which places this state at 1.06 MeV. In our calculation, the ground state of ^{31}F is an extremely mixed $\frac{5}{2}^+$ (66% intruder) and the excited $\frac{1}{2}^+$ (74% intruder) appears at much lower excitation energy, 0.21 MeV. Neutron excitations result in binding energy gains of 1.9 and 2.5 MeV, respectively, which may help to explain the far off location of the fluorine neutron drip line.

E. ^{33}Al and ^{35}Al

^{33}Al has its ground states largely dominated by the "normal" configurations (~80%). Thus, it does not belong properly to the island of inversion. The calculations reproduce very

well the properties of the $\frac{5}{2}^+$ ground state; the magnetic moment is $+4.088(5)\mu_N$ vs $+4.17\mu_N$ (b) and $+3.86\mu_N$ (e); the spectroscopic quadrupole moment is +0.12 eb compared to the calculated +0.12 eb. Our results do not produce a low lying $\frac{5}{2}^+$ as surmised in the experiment of Ref. [41]. This is consistent with the large excitation energy of the intruder 0^+ in ^{34}Si. The lowest excited state is predicted to be a $\frac{5}{2}^+$ of intruder nature at 1.70 MeV followed by two other 2p-2h states at 1.85 MeV ($\frac{1}{2}^+$) and 2.28 MeV($\frac{5}{2}^+$). Contrary to some compiled results we do not produce negative parity states in this range of energies. In the $\frac{5}{2}^+$ ground state of ^{35}Al the "normal" configurations still lead, but barely so at 52%. The lowest excited states, $\frac{1}{2}^+$ at 0.63 MeV and $\frac{3}{2}^+$ at 0.80 MeV, are intruders.

F. The limits of the "big island of deformation"

We argued already that the previously established $N = 20$ and $N = 28$ islands of inversion or deformation merge in the neon, sodium, and magnesium isotopic chains, creating a bigger one (big island of deformation, or BID). Referring only to the ground states, their $N = 19$ isotopes seem to belong to it as well, and their $N = 18$ ones not (but see below). The value $N = 31$ and the neutron drip line define the west shore of the BID. Some heavy aluminums, silicons ($N \geqslant 26$), phosphors, and sulfurs ($N \geqslant 28$) do belong to the $N = 28$ sector of the BID as well, but their less neutron rich isotopes do not belong to the $N = 20$ sector (except perhaps ^{34}Al). Fluorines are transitional, as we have just discussed. Of the $N = 18$ isotones, only ^{28}Ne and ^{29}Na can pretend to pertain to it with 50% and 40% of intruder components in their ground states. For the other isotopes, although the ground states are "normal," quite often intruder states show up at low excitation energy.

VII. CONCLUSIONS

We showed that the model space comprising the sd shell for the protons and the sd-pf shell for the neutrons, together with the effective interaction SDPF-U-MIX, make it possible to describe a very large region of nuclei, in particular the very neutron rich nuclei at or around the $N = 20$ "islands of inversion." In many cases the inversion of configurations produces deformed ground state bands, hence we use the term "islands of deformation" as well. According to our calculations (and also to the meager experimental data available), the two islands merge in the magnesium chain. In the calculations they also merge in the neon and sodium chains. However, this could only be checked experimentally if their neutron drip lines happened to be close enough to $N = 28$. We studied in detail the mechanisms that lead to the inversion of normal and intruder configurations, paying particular attention to the properties of the states at fixed np-nh configurations and to their correlation energy gains. We compared the calculations to some selected experimental results. The ubiquitous deformed bands have intrinsic (electric) quadrupole moments in the range $Q_0 = 60$–$80\ e\ \mathrm{fm}^2$. We leave for the future a full scan of the region with the SDPF-U-MIX interaction, as well as the study of the one and two neutron separation energies, which requires some extra monopole work, probably including three-body terms.

ACKNOWLEDGMENTS

This work was partially supported by the MICINN (Spain) (Grant No. FPA2011-29854), by the IN2P3 (France) and MICINN (Spain) (Grant No. AIC11-D-648), and by the Comunidad de Madrid (Spain) (Grant No. HEPHACOS S2009-ESP-1473). A.P. is supported by MINECOs (Spain) Centro de Excelencia Severo Ochoa Programme under Grant No. SEV-2012-0249.

APPENDIX: THE SDPF-U-MIX INTERACTION

The SDPF-U-SI interaction was designed for $0\hbar\omega$ calculations of very neutron rich sd nuclei around $N = 28$ in a valence space comprising the full sd (pf) shell for the protons (neutrons); i.e., this interaction was defined (implicitly) with a core of ^{28}O. Its single particle energies (SPEs) and monopoles (neutron-proton sd-pf and neutron-neutron pf-pf) were fixed by the spectra of ^{35}Si, ^{41}Ca, ^{47}K, and ^{49}Ca. To allow for the mixing among different np-nh neutron configurations across $N = 20$, it is necessary to add to SDPF-U-SI the following new ingredients: (a) We take the off-diagonal cross shell sd-pf matrix elements from the Lee-Kahana-Scott G matrix [42] scaled as in Ref. [24]. (b) We take the SPEs on a core of ^{16}O: for the the sd-shell orbits we use always the USD values [17], while for the pf-shell orbits we have no experimental guidance at all. Nonetheless, for any particular set of pf-shell SPEs, the neutron-neutron sd-pf monopoles must be chosen so as to reproduce the spectrum of ^{35}Si and the $N = 20$ gap. Because the solution is not unique, we anchored our choice to obtain a reasonable energy for the first excited 0^+ state in ^{30}Mg. This guarantees that in our isotopic course toward $N = 20$ the descent of the intruder states proceeds with the correct slope. (c) We incorporate into the isovector pairing of the sd shell the same modifications introduced in Ref. [8]. The pairing reduction is needed to avoid double counting when core excitations are taken explicitly into account. A recent study of the effects of the change of the reference valence space in the calculation of the renormalizations of the sd and pf matrix elements, made in Ref. [43], gives a robust foundation to these modifications.

A concern may arise about the applicability of this valence space and the interaction SDPF-U-MIX to nuclei with $Z >$ 16. Indeed, without treating properly the proton excitations, a description of the argon and calcium isotopes close to $N =$ 20 is excluded. Therefore, it would be premature to give an answer before they are incorporated in the model. We expect the neutron core excitations to do part of the work in the sulfur isotopes near $N = 20$, but their effects should be somehow blocked toward $N = 28$.

The very large span in neutron number that this interaction has to cope with brings in some global monopole problems which can be solved by adding to the Hamiltonian (minute) two- plus three-body monopole terms of the form

$\frac{1}{2}N(N-1)V_2$ or $\frac{1}{6}N(N-1)(N-2)V_3$ with $N = A - 16$, which do not affect the spectroscopic results. We have not yet completed this part of the task that would make it possible to obtain predictions for the neutron separation energies.

[1] I. Talmi and I. Unna, Phys. Rev. Lett. **4**, 469 (1960).

[2] C. Thibault *et al.*, Phys. Rev. C **12**, 644 (1975); G. Huber *et al.*, *ibid.* **18**, 2342 (1978); C. Détraz *et al.*, *ibid.* **19**, 164 (1979); D. Guillemaud-Mueller *et al.*, Nucl. Phys. A **426**, 37 (1984); P. Baumann *et al.*, Phys. Lett. B **228**, 458 (1989).

[3] T. Motobayashi *et al.*, Phys. Lett. B **346**, 9 (1995); H. Iwasacki *et al.*, *ibid.* **522**, 227 (2001); B. V. Pritychenko *et al.*, Phys. Rev. C **63**, 011305(R) (2000); Y. Yanagisawa *et al.*, Phys. Lett. B **566**, 84 (2003); J. A. Church *et al.*, Phys. Rev. C **72**, 054320 (2005).

[4] G. Neyens *et al.*, Phys. Rev. Lett. **94**, 022501 (2005); D. T. Yordanov *et al.*, *ibid.* **99**, 212501 (2007); P. Himpe *et al.*, Phys. Lett. B **658**, 203 (2008); R. Kanungo *et al.*, *ibid.* **685**, 253 (2010); G. Neyens, Phys. Rev. C **84**, 064310 (2011).

[5] H. Mach *et al.*, Phys. Lett. B **230**, 21 (1989); R. W. Ibbotson *et al.*, Phys. Rev. Lett. **80**, 2081 (1998); Ch. Hofmann *et al.*, Phys. Rev. C **42**, 2632 (1990); S. Nummela *et al.*, *ibid.* **64**, 054313 (2001); N. Iwasa *et al.*, *ibid.* **67**, 064315 (2003); A. Gade *et al.*, Phys. Rev. Lett. **99**, 072502 (2007); K. Wimmer *et al.*, **105**, 252501 (2010); N. Hinohara *et al.*, Phys. Rev. C **84**, 061302 (2011).

[6] X. Campi *et al.*, Nucl. Phys. A **251**, 193 (1975).

[7] A. Poves and J. Retamosa, Phys. Lett. B **184**, 311 (1987); E. K. Warburton, J. A. Becker, and B. A. Brown, Phys. Rev. C **41**, 1147 (1990); K. Heyde and J. L. Wood, J. Phys. G **17**, 135 (1991); N. Fukunishi, T. Otsuka, and T. Sebe, Phys. Lett. B **296**, 279 (1992).

[8] Y. Utsuno *et al.*, Phys. Rev. C **60**, 054315 (1999); T. Otsuka *et al.*, Prog. Part. Nucl. Phys. **47**, 319 (2001).

[9] E. Caurier *et al.*, Phys. Rev. C **58**, 2033 (1998); J. L. Wood *et al.*, Nucl. Phys. A **651**, 323 (1999); E. Caurier *et al.*, *ibid.* **693**, 374 (2001); B. A. Brown, Prog. Part. Nucl. Phys. **47**, 517 (2001); E. Caurier *et al.*, Eur. Phys. J. A **15**, 145 (2002).

[10] J. Terasaki, H. Flocard, P.-H. Heenen, and P. Bonche, Nucl. Phys. A **621**, 706 (1997); P. G. Reinhard, D. J. Dean, W. Nazarevicz, J. Dobaczewski, J. A. Maruhn, and M. R. Strayer, Phys. Rev. C **60**, 014316 (1999); G. A. Lalazissis, D. Vretenar, P. Ring, M. Stoisov, and L. Robledo, Nucl. Phys. A **60**, 014310 (1999); S. Peru *et al.*, Eur. Phys. J. A **9**, 35 (2000); R. Rodriguez-Guzman, J. L. Egido, and L. M. Robledo, Phys. Rev. C **65**, 024304 (2002).

[11] F. Nowacki and A. Poves, Phys. Rev. C **79**, 014310 (2009).

[12] B. Bastin *et al.*, Phys. Rev. Lett. **99**, 022503 (2007).

[13] S. Takeuchi *et al.*, Phys. Rev. Lett. **109**, 182501 (2012).

[14] J. Fridmann *et al.*, Nature (London) **435**, 922 (2005); A. Gade *et al.*, Phys. Rev. C **71**, 051301(R) (2005); S. Grevy *et al.*, Eur. Phys. J. A **25**, 111 (2005); J. Fridmann *et al.*, Phys. Rev. C **74**, 034313 (2006); B. Jurado *et al.*, Phys. Lett. B **649**, 43 (2007); L. Gaudefroy *et al.*, Phys. Rev. Lett. **97**, 092501 (2006); A. Gade *et al.*, Phys. Rev. C **74**, 034322 (2006); C. M. Campbell *et al.*, Phys. Rev. Lett. **97**, 112501 (2006); Phys. Lett. B **652**, 169 (2007).

[15] L. Gaudefroy *et al.*, Phys. Rev. Lett. **102**, 092501 (2009); M. De Rydt *et al.*, Phys. Rev. C **81**, 034308 (2010); C. Force *et al.*, Phys. Rev. Lett. **105**, 102501 (2010); D. Santiago-Gonzalez *et al.*, Phys. Rev. C **83**, 061305(R) (2011).

[16] Y. Utsuno *et al.*, Phys. Rev. C **86**, 051301 (2012).

[17] B. A. Brown and B. H. Wildenthal, Annu. Rev. Nucl. Part. Sci. **38**, 29 (1988).

[18] E. Caurier, G. Martínez-Pinedo, F. Nowacki, A. Poves, and A. P. Zuker, Rev. Mod. Phys. **77**, 427 (2005).

[19] A. P. Zuker, J. Retamosa, A. Poves, and E. Caurier, Phys. Rev. C **52**, R1741 (1995).

[20] A. Arima, M. Harvey, and K. Shimizu, Phys. Lett. B **30**, 517 (1969); K. Hecht and A. Adler, Nucl. Phys. A **137**, 129 (1969).

[21] J. P. Elliott, Proc. R. Soc. London, Ser. A **245**, 128 (1956).

[22] C. E. Svensson *et al.*, Phys. Rev. Lett. **85**, 2693 (2000).

[23] E. Ideguchi *et al.*, Phys. Rev. Lett. **87**, 222501 (2001).

[24] E. Caurier, J. Menéndez, F. Nowacki, and A. Poves, Phys. Rev. C **75**, 054317 (2007).

[25] M. Dufour and A. P. Zuker, Phys. Rev. C **54**, 1641 (1996).

[26] M. Seidlitz *et al.*, Phys. Lett. B **700**, 181 (2011).

[27] V. Tripathi *et al.*, Phys. Rev. C **77**, 034310 (2008).

[28] P. Doornenbal *et al.*, Phys. Rev. Lett. **111**, 212502 (2013).

[29] W. A. Richter, S. Mkhize, and B. A. Brown, Phys. Rev. C **78**, 064302 (2008).

[30] J. R. Terry *et al.*, Phys. Rev. C **77**, 014316 (2008).

[31] P. Doornenbal *et al.*, Phys. Rev. Lett. **103**, 032501 (2009).

[32] T. Nakamura *et al.*, Phys. Rev. Lett. **103**, 262501 (2009); M. Takechi *et al.*, Phys. Lett. B **707**, 357 (2012).

[33] A. Poves *et al.*, Phys. Scr. **T150**, 014030 (2012).

[34] F. Rotaru *et al.*, Phys. Rev. Lett. **109**, 092503 (2012).

[35] G. Klotz *et al.*, Phys. Rev. C **47**, 2502 (1993).

[36] C. M. Mattoon *et al.*, Phys. Rev. C **75**, 017302 (2007).

[37] S. Takeuchi *et al.*, Phys. Rev. C **79**, 054319 (2009).

[38] P. Doornenbal *et al.*, Phys. Rev. C **81**, 041305(R) (2010).

[39] A. Gade *et al.*, Phys. Rev. C **83**, 044305 (2011).

[40] H. Sakurai, Astrophysics and Nuclear Structure: International Workshop XLI on Gross Properties of Nuclei and Nuclear Excitations, Hirschegg, Austria, 2013 (unpublished).

[41] W. Mittig *et al.*, Eur. Phys. J. A **15**, 157 (2002).

[42] S. Kahana, H. Lee, and C. Scott, Phys. Rev. **185**, 1378 (1969).

[43] K. Sieja and F. Nowacki, Nucl. Phys. A **857**, 9 (2011).